

Discovery of Novel Sertraline Derivatives as Potent Anti-*Cryptococcus* AgentsWang Li,[§] Zhaolin Yun,[§] Changjin Ji, Jie Tu, Wanzhen Yang, Jian Li,^{*} Na Liu,^{*} and Chunquan Sheng^{*}Cite This: *J. Med. Chem.* 2022, 65, 6541–6554

Read Online

ACCESS |



Metrics & More

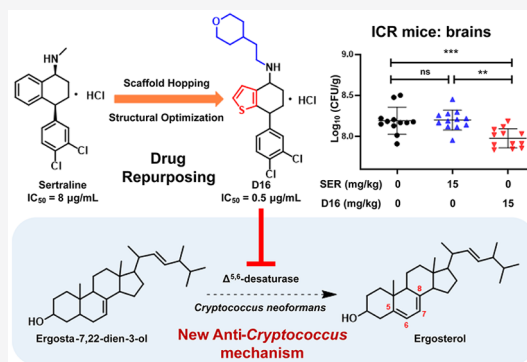


Article Recommendations



Supporting Information

ABSTRACT: Treatment of life-threatening cryptococcal meningitis (CM) is highly challenging due to the limited efficacy of the available antifungal drugs. Antidepressant sertraline (SER) has been proposed to be a potential antifungal agent for CM. However, clinical studies indicated that SER failed to achieve the expected therapeutic effects. Herein, novel SER derivatives were designed by scaffold hopping, and they showed improved anticryptococcal activity both *in vitro* and *in vivo*. In particular, compound **D16** was identified as a promising anti-CM agent with a new antifungal mode of action. It acted by blocking the biosynthesis of ergosterol through the inhibition of $\Delta^{5,6}$ -desaturase. This study provides a new target and a drug-like candidate for CM treatment.



INTRODUCTION

Contrary to the continuous improvement of medical and health conditions, fungal infections have increasingly become a global public health problem.¹ *Candida*, *Aspergillus*, *Cryptococcus*, and *Pneumocystis* account for ~90% of the pathogens that cause fungal infections.^{2–4} Cryptococcal infections are associated with high morbidity and mortality, particularly in immunocompromised patients.^{5,6} The main clinical symptom of cryptococcosis is lethal meningoencephalitis, which causes ~200000 deaths annually.^{7,8} The treatment of cryptococcal meningitis (CM) recommended by the World Health Organization (WHO) is the combination of amphotericin B (AmB) with 5-flucytosine (5-FU) or an alternative combinational therapy of fluconazole (FLC) with 5-FU.^{9,10} However, toxicity, drug resistance, and limited efficiency restricted the applications of existing drugs in the clinic.^{11–13} Despite the clinical requirements, no new class of CM therapeutic drug has reached the market in the past two decades.^{14,15} Thus, there is an urgent need to identify new targets and new lead compounds for CM.

Drug repurposing has the advantages of a high success rate, a short development time, and a low cost from bench to bedside because the chemical skeleton of marketed drugs is highly likely to become a drug.^{16–19} Antidepressant sertraline (SER), a selective serotonin transporter (SERT) inhibitor, was recently repositioned to be a potential antifungal agent.^{20–22} However, the inhibitory activity of SER against *Cryptococcus neoformans* H99 is moderate ($IC_{50} = 8 \mu\text{g/mL}$), which was mainly evaluated as a combinational antifungal therapy.²³ In a clinical trial (NCT01802385), daily treatment with 200 mg of SER did not reduce the mortality in CM patients.^{23,24} In addition, the antifungal mechanism of SER remains to be verified, although its

antifungal activity was proposed to be associated with the inhibition of the efflux pump, fungal metabolism, protein synthesis, cell membrane phospholipid synthesis, etc.^{20,25–27}

To improve the anticryptococcal activity of SER, herein, a series of novel SER derivatives were designed by scaffold hopping. Among them, compound **D16** showed better *in vitro* and *in vivo* activity than SER. Interestingly, compound **D16** acted by a new antifungal mechanism, which effectively blocked the biosynthesis of ergosterol through the inhibition of $\Delta^{5,6}$ -desaturase.

RESULTS AND DISCUSSION

SER Isomers Showed Similar Antifungal Activity. The structure of SER contains two chiral centers. However, the antifungal activity of the SER isomers is still unknown. Thus, *cis*-SER (*SS* configuration) and *trans*-SER (*RR* configuration) were separated according to the reported method (Figure 1).^{28,29} An *in vitro* antifungal activity assay showed that the IC_{50} values of SER, *cis*-SER, and *trans*-SER against *C. neoformans* H99 were all $8 \mu\text{g/mL}$, suggesting that the chiral centers had little effect on antifungal activity. Considering the difficulty of synthesis and separation, herein SER derivatives were synthesized in the form of racemates without further chiral resolution.

Received: October 26, 2021

Published: March 6, 2022



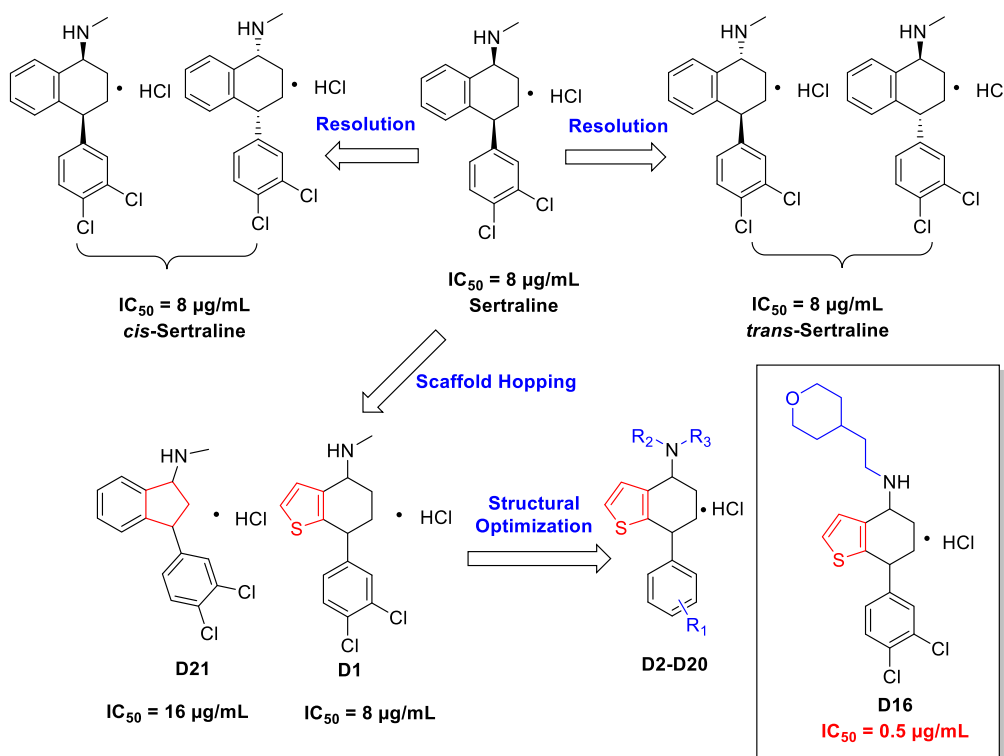


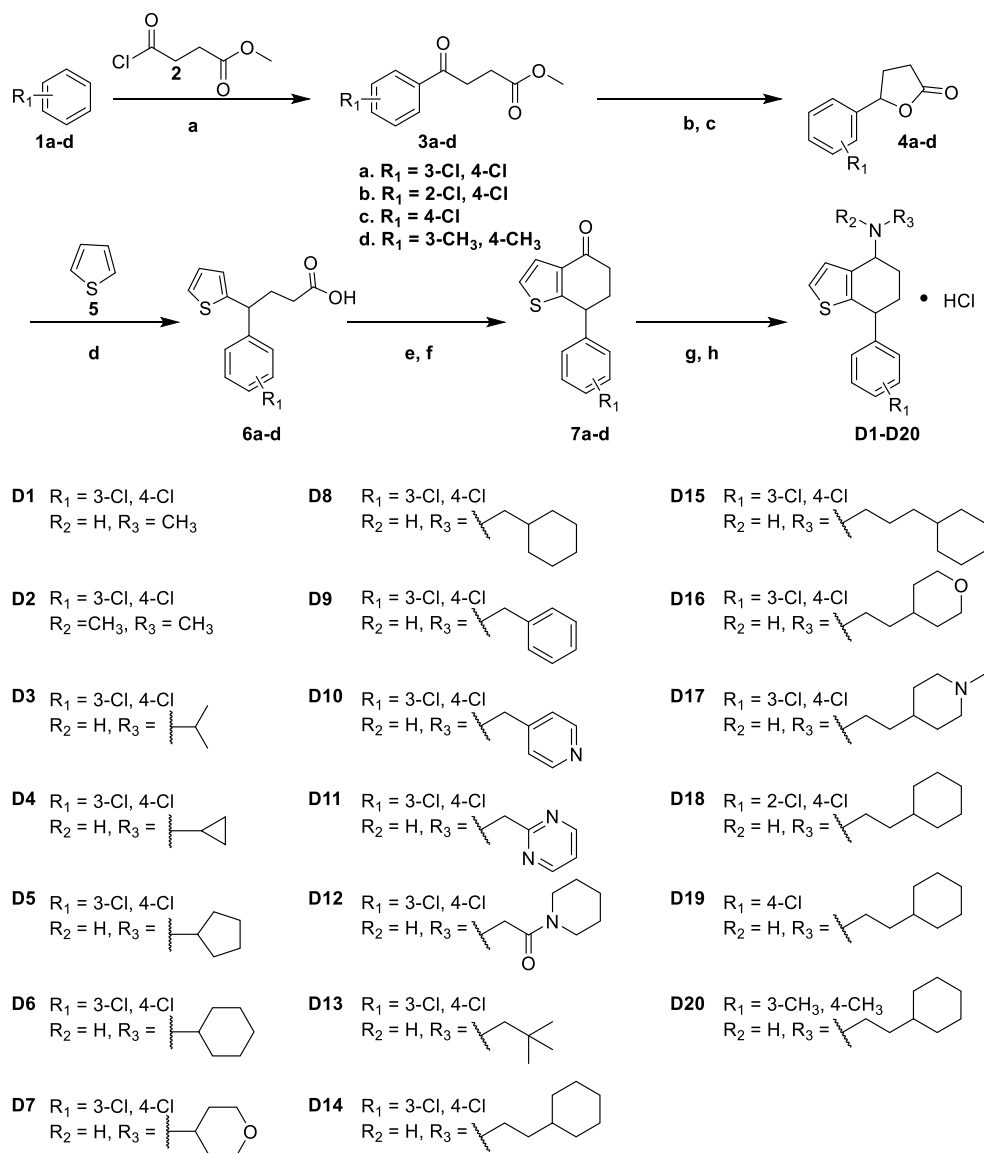
Figure 1. Resolution of SER and design strategies of SER derivatives.

Rationale for the Design of SER Derivatives. Previous structure–activity relationship (SAR) studies indicated that the benzo-cyclohexane scaffold of SER is necessary for the affinity of binding to SERT.³⁰ Moreover, the substitutions on the tetrahydronaphthalene scaffold of SER have been extensively explored.³¹ To reduce the activity toward SERT, herein, scaffold hopping of SER was investigated using benzothiophene (**D1**) and 2,3-dihydro-1*H*-indene (**D21**) to replace the tetrahydronaphthalene pharmacophore. Compared with that of SER, the antifungal activity of compound **D1** was maintained (for *C. neoformans* H99, $IC_{50} = 8 \mu\text{g/mL}$), whereas compound **D21** showed lower activity ($IC_{50} = 16 \mu\text{g/mL}$). Therefore, new derivatives with various amine and phenyl substitutions on the benzothiophene scaffold of compound **D1** were designed [**D1**–**20** (Figure 1)].

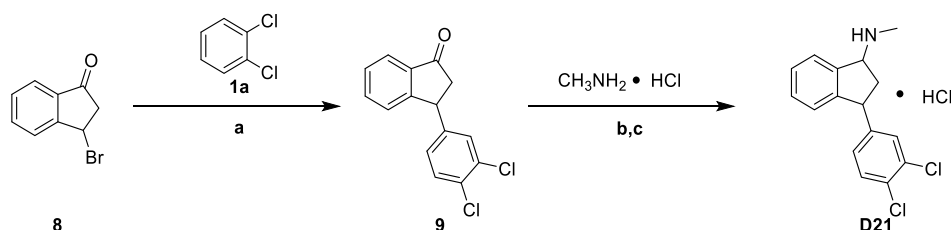
Chemistry. The chemical synthesis of the SER derivatives is depicted in Schemes 1 and 2. Intermediates **3a–d** were synthesized from commercially available substituted benzene and methyl 4-chloro-4-oxobutrate by the Friedel–Crafts acylation reaction. Then, intermediates **3a–d** were reduced in the presence of NaBH_4 , followed by reaction with trifluoroacetic acid to form intermediates **4a–d**. They reacted with thiophene (**5**) by the Friedel–Crafts alkylation reaction to afford intermediates **6a–d**, which were treated with SOCl_2 , and then directly subjected to the intramolecular Friedel–Crafts acylation reaction to obtain intermediates **7a–d**. Finally, various amines reacted with intermediates **7a–d** by the reductive amination reaction, and the products were further treated with ether hydrochloride to give target compounds **D1–20** as racemates. Intermediate **9** was obtained from 3-bromo-1-indanone (**8**) and 1,2-dichlorobenzene by the Friedel–Crafts alkylation reaction. Target compound **D21** was prepared by a procedure similar to that for compounds **D1–20** (Scheme 2).

In Vitro Antifungal Activities and SARs. As shown in Table 1, the addition of an *N*-methyl group to compound **D1** led to obviously decreased activity (for compound **D2**, $IC_{50} = 32 \mu\text{g/mL}$). The replacement of the *N*-methyl group with isopropyl (compound **D3**), cyclopropyl (compound **D4**), cyclopentyl (compound **D5**), or hexamethylene (compound **D6**) resulted in comparable or slightly decreased antifungal activity. In contrast, tetrahydropyran substitution was favorable for the antifungal activity (for compound **D7**, $IC_{50} = 4 \mu\text{g/mL}$). The insertion of one carbon atom between the hexamethylene group and the nitrogen atom of compound **D6** led to improved antifungal activity (for compound **D8**, $IC_{50} = 2 \mu\text{g/mL}$). However, further replacement of the hexamethylene group with phenyl, heterocyclic, or alkyl groups (compounds **D9–13**) had a negative impact on antifungal activity. Interestingly, further extension of the *N*-side chain was favorable for improving the antifungal activity (for compound **D14**, $IC_{50} = 1 \mu\text{g/mL}$). Further variation of the 2,4-dichlorophenyl group of compound **D14** generally caused reduced potency (compounds **D18–20**). Finally, the best compound in this series (for compound **D16**, $IC_{50} = 0.5 \mu\text{g/mL}$) was obtained by insertion of an oxygen atom into the hexamethylene group of compound **D14**.

Compound D16 Effectively Inhibited the Growth of *C. neoformans* H99. Due to the potent inhibitory activity of compounds **D14** and **D16** against *C. neoformans* H99, they were further evaluated by the time–growth curve assay (Figure 2A). FLC showed moderate activity in inhibiting the growth of *C. neoformans* H99 at low and high concentrations. SER significantly inhibited the growth of *C. neoformans* H99 at 8 $\mu\text{g/mL}$. At a concentration of 8 or 4 $\mu\text{g/mL}$, compound **D14** effectively inhibited the growth of *C. neoformans* H99 during the initial stage (3–48 h). However, the inhibitory potency of compound **D14** decreased obviously after 48 h. Interestingly, compound **D16** almost completely inhibited the growth of *C.*

Scheme 1^a

^aReagents and conditions: (a) AlCl_3 , DCM, rt, N_2 , 3 h, 68.9–83.5% yield; (b) NaBH_4 , MeOH, 0 °C, 1 h, 83.3–91.4% yield; (c) TFA, DCM, rt, 2 h, 78.9–88.5% yield; (d) AlCl_3 , DCM, rt, N_2 , 5 h, 48.0–65.2% yield; (e) SOCl_2 , DMF, DCM, rt, 3 h, 62.1–69.7% yield; (f) AlCl_3 , DCM, rt, N_2 , 3 h, 30.1–39.2% yield; (g) NaBH_3CN , $\text{Ti}(\text{OPr-}i)_4$, MeOH, 40 °C, overnight; (h) $\text{HCl}/\text{Et}_2\text{O}$, rt, 1 h (total yield of steps g and h of 15.5–47.7%).

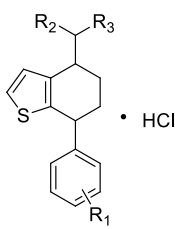
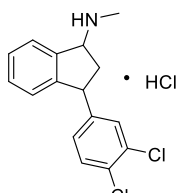
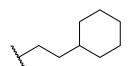
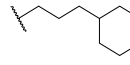
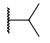
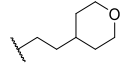
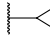
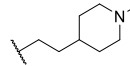
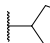
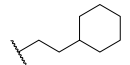
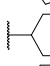
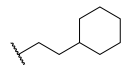
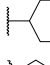
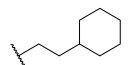


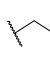
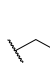


Scheme 2^a

^aReagents and conditions: (a) AlCl_3 , DCM, rt, N_2 , overnight, 37.1% yield; (b) NaBH_3CN , $\text{Ti}(\text{OPr-}i)_4$, MeOH, 40 °C, overnight; (c) $\text{HCl}/\text{Et}_2\text{O}$, rt, 1 h (total yield of steps b and c of 10.8%).

neoformans H99 at 8 $\mu\text{g}/\text{mL}$, and the inhibition rate remained at nearly 100% after 72 h. At a lower concentration (1 $\mu\text{g}/\text{mL}$), compound **D16** inhibited the growth of *C. neoformans* H99 better than SER. The time–growth curve suggested that compound **D16** possessed good potency against *C. neoformans*

H99 growth, which was more active than FLC and SER. To verify whether compound **D16** had a fungicidal effect, we carried out the time–fungicidal curve assay. As shown in Figure 2B, FLC did not show a fungicidal effect at a concentration of 8 $\mu\text{g}/\text{mL}$, which was consistent with the literature results.³² The

Table 1. *In Vitro* Antifungal Activities of SER Derivatives D1–21 against *C. neoformans* H99 (IC₅₀, micrograms per milliliter, 72 h)

 D1-D20					 D21				
Compounds	R ₁	R ₂	R ₃	IC ₅₀	Compounds	R ₁	R ₂	R ₃	IC ₅₀
D1	3-Cl, 4-Cl	H	CH ₃	8	D14	3-Cl, 4-Cl	H		1
D2	3-Cl, 4-Cl	CH ₃	CH ₃	32	D15	3-Cl, 4-Cl	H		2
D3	3-Cl, 4-Cl	H		16	D16	3-Cl, 4-Cl	H		0.5
D4	3-Cl, 4-Cl	H		16	D17	3-Cl, 4-Cl	H		2
D5	3-Cl, 4-Cl	H		8	D18	2-Cl, 4-Cl	H		4
D6	3-Cl, 4-Cl	H		8	D19	4-Cl	H		64
D7	3-Cl, 4-Cl	H		4	D20	3-CH ₃ , 4-CH ₃	H		32
D8	3-Cl, 4-Cl	H		2	D21	-	-	-	16
D9	3-Cl, 4-Cl	H		32	SER	-	-	-	8
D10	3-Cl, 4-Cl	H		16	FLC	-	-	-	2
D11	3-Cl, 4-Cl	H		32	AmB	-	-	-	0.25
D12	3-Cl, 4-Cl	H		8	5-FU	-	-	-	2
D13	3-Cl, 4-Cl	H		4					

minimum fungicidal concentrations (MFCs) of AmB, SER, and compound **D16** were 4, 16, and 8 $\mu\text{g/mL}$, respectively.

Compounds D14 and D16 Significantly Inhibited Biofilm Formation. The formation of fungal biofilms is the main factor of colonization on the surface of organs,^{33,34} which is closely related to recurrent fungal infection and drug resistance.³⁵ The inhibitory effects of compounds **D14** and **D16** against the formation of *C. neoformans* H99 biofilms were investigated. As shown in panels A and B of Figure 3, FLC showed modest activity in inhibiting the formation of *C. neoformans* H99 biofilms (~50% inhibition rate at 8 $\mu\text{g/mL}$), while SER significantly inhibited the formation of fungal biofilms only at a high concentration (8 $\mu\text{g/mL}$). In contrast, compounds **D14** and **D16** effectively inhibit the formation of *C. neoformans* H99 biofilms in a concentration-dependent manner. At 2 $\mu\text{g/mL}$, an ~50% inhibition rate was achieved after the treatment of compounds **D14** and **D16**. When the concentration was increased to 8 $\mu\text{g/mL}$, the formation of *C. neoformans* H99 biofilms was completely inhibited (Figure 3C,D). Thus, compounds **D14** and **D16** exhibited good activity against the formation of *C. neoformans* H99 biofilms.

Compound D16 Showed Selective Anti-*Cryptococcus* Activity. On the basis of the *in vitro* antifungal and antibiofilm activity, compound **D16** was selected for further evaluation. To investigate the antifungal spectrum, inhibitory activities of SER and compound **D16** against various drug-resistant and -sensitive *Candida albicans*, *Candida tropicalis*, *Candida glabrata*, *Candida krusei*, *Candida auris*, and *Aspergillus fumigates* were tested. Both SER and compound **D16** showed moderate to weak antifungal activity (IC₅₀ range of 8–64 $\mu\text{g/mL}$) against these tested strains (Table 2). These results suggested that SER and its derivative **D16** showed selective anti-*Cryptococcus* activity. Furthermore, the anti-*Cryptococcus* activity of compound **D16** against 50 strains of *Cryptococcus* was also performed (Table S1). The IC₅₀ range of compound **D16** against *Cryptococcus* was 0.06–2 $\mu\text{g/mL}$ with a MIC₅₀ value (average IC₅₀ values) of 0.62 $\mu\text{g/mL}$ (Table 3). The results further confirmed that compound **D16** was more potent than FLC (MIC₅₀ = 1.14 $\mu\text{g/mL}$) and SER (MIC₅₀ = 3.6 $\mu\text{g/mL}$). The MFC/MIC ratio of compound **D16** was 7.47, indicating that compound **D16** had a fungistatic effect (Table S2).

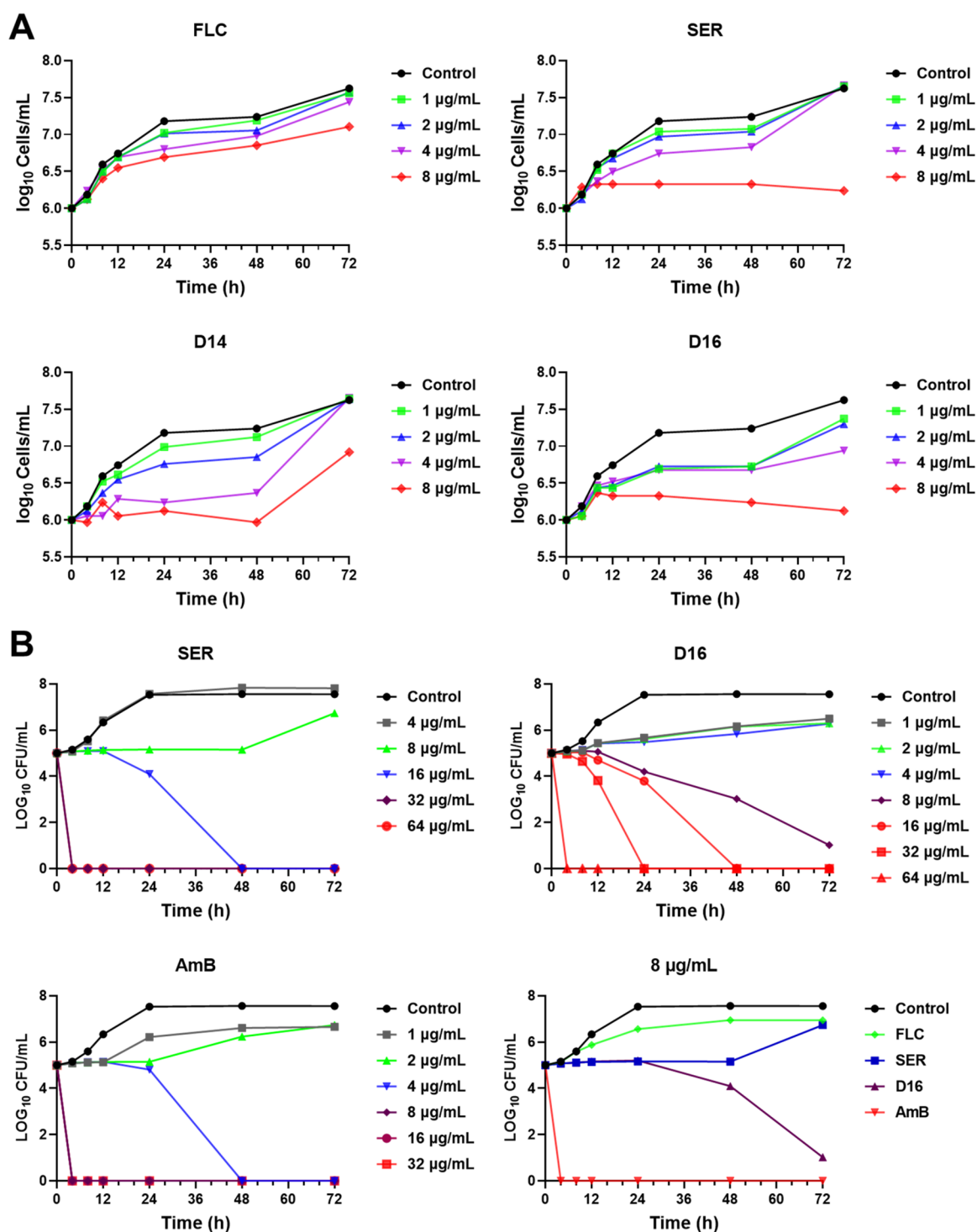


Figure 2. Growth inhibitory potency of FLC, SER, D14, and D16 against *C. neoformans* H99. (A) Time–growth curve assay. Starting at a density of 1×10^6 cells/mL, the inhibitory effect against *C. neoformans* H99 at different concentrations was evaluated. (B) Time–fungicidal curve at different concentrations of FLC, SER, AmB, and D16 against *C. neoformans* H99. The colony-forming units (CFU) of *C. neoformans* H99 cells were counted at 0, 4, 8, 12, 24, 48, and 72 h.

Compound D16 Showed Potent *In Vivo* Anti-Cryptococcal Efficacy. Initially, the stability and cytotoxicity of compound D16 were investigated. Compound D16 showed good *in vitro* metabolic stability in liver microsomes with low cytotoxicity against a human HUVEC cell line (Table 4). Moreover, a parallel artificial membrane permeation assay (PAMPA) was used to test the permeability of the blood–brain barrier (BBB) to compound D16. Compound D16 could

penetrate the BBB at a level comparable to that of SER (Table S3). Thus, the *in vivo* anticryptococcal potency of compound D16 was further evaluated. The mouse model of CM was established by tail vein injection of *C. neoformans* H99. Compound D16 and SER were given by intragastric administration at a 15 mg/kg dose daily. The fungal burden of mouse brain was further performed. Compared with the saline group, compound D16 significantly reduced the number of *C.*

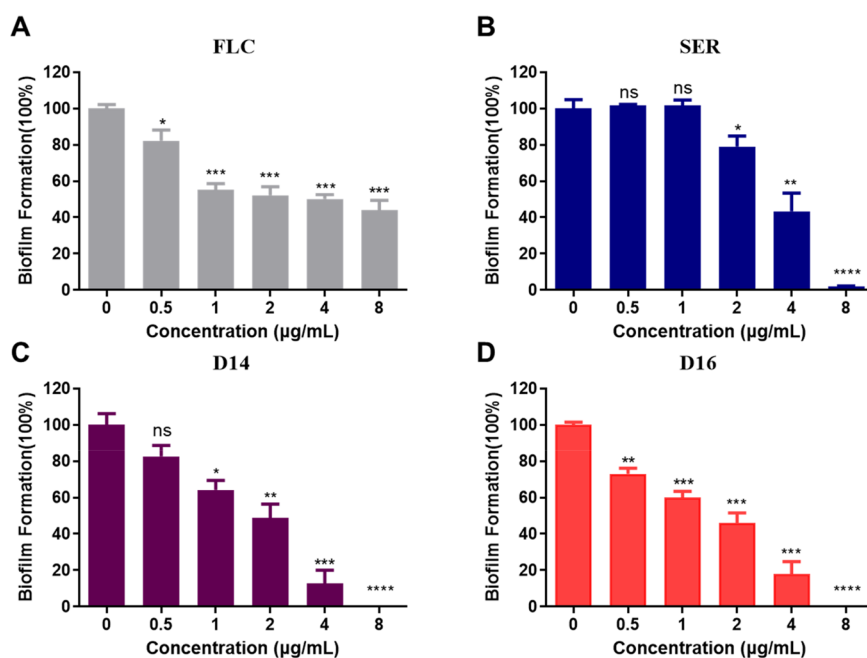


Figure 3. Inhibitory potency of (A) FLC, (B) SER, (C) D14, and (D) D16 at different concentrations against the formation of *C. neoformans* H99 biofilms determined by the XTT reduction assay. OD₄₉₀ values were measured, and standard deviations (SDs) from three parallel experiments. **P* < 0.05, ***P* < 0.01, ****P* < 0.001, and *****P* < 0.0001 vs DMSO.

Table 2. Antifungal Spectrum of Compound D16 (IC₅₀, micrograms per milliliter, 48 h)

species	strain	FLC	SER	D16
<i>C. albicans</i>	SC5314	0.25	32	32
<i>C. albicans</i>	904	>64	32	32
<i>C. albicans</i>	0304103	>64	32	32
<i>C. tropicalis</i>	10186	>64	16	32
<i>C. glabrata</i>	9073	64	64	32
<i>C. glabrata</i>	9025	16	16	8
<i>C. krusei</i>	10153	64	8	8
<i>C. auris</i>	0029	>64	16	16
<i>C. auris</i>	0030	>64	8	8
<i>C. auris</i>	15448	4	4	8
<i>A. fumigates</i>	7544	>64	8	32
<i>A. fumigates</i>	023-2	>64	8	32

Table 3. Antifungal Activity of Compound D16 against 50 *Cryptococcus* Strains (micrograms per milliliter, 72 h)

	FLC	AmB	SER	D16
IC ₅₀ range	0.13–4	0.03–0.25	0.25–8	0.06–2
MIC ₅₀	1.14	0.13	3.6	0.62

Table 4. Metabolic Stabilities in Mouse Liver Microsomes and Cytotoxicities of Compound D16 and SER

compound	<i>T</i> _{1/2} ^a (min)	CL ^b (mL min ^{−1} mg ^{−1})	HUVEC (IC ₅₀ , μM)
D16	40.11	136.07	20.18
SER	41.47	131.59	19.18
ketanserin	20.12	271.28	—

^aHalf-life. ^bClearance.

neoformans H99 cells in the brain after 5 days. At the same dosage, SER was unable to exert significant *in vivo* antifungal activity (Figure 4A). This result was consistent with the fact that SER alone could not reduce the mortality in the clinical trial

(NCT 01802385).²³ The survival time assay was performed to further evaluate the *in vivo* potency of compound D16 in the mouse model of CM. As shown in Figure 4B, compound D16 could significantly prolong the median survival time (14 days) of the infected mice at a dose of 15 mg/kg. In contrast, there was no significant difference between the SER group and the blank control [11.5 and 11 days, respectively (*P* > 0.05)].

Compound D16 Destroyed Fungal Cell Membranes.

Compound D16 showed obvious anticytotoxic activity both *in vitro* and *in vivo*. However, as a novel anticytotoxic agent, the mechanism of action of compound D16 remains unknown. To further explore the antifungal mechanisms, a transmission electron microscope assay was carried out to observe the injury of *C. neoformans* H99 cells at different concentrations of compound D16 and SER. Normal *C. neoformans* H99 cells had a uniform density and a clear outline. The *C. neoformans* H99 cells treated with 4 μg/mL SER could not distinguish the damaged area clearly. After the treatment with compound D16, the membrane of *C. neoformans* H99 was damaged in a concentration-dependent manner (Figure 5), which was consistent with the results from the time–fungicidal curve (Figure 2). In addition, as the concentration of compound D16 was increased, the cell membranes of *C. neoformans* H99 cells were gradually blurred, leading to the complete rupture of the cell membrane and efflux of cell contents at 4 μg/mL (Figure 5). Thus, compound D16 killed the *C. neoformans* H99 cells by destroying the integrity of fungal cell membranes.

Compound D16 Acted on the Ergosterol Synthesis Pathway of *C. neoformans* H99 by Inhibiting Δ^{5,6}-Desaturase. A transmission electron microscope assay revealed that the cell membrane of *C. neoformans* H99 was damaged by treatment with compound D16. Ergosterol is a major component of fungal cell membrane integrity.^{36–38} To validate whether compound D16 acted on the ergosterol synthesis pathway, we further analyzed the sterol contents of the *C. neoformans* H99 cytomembrane by gas chromatography–mass

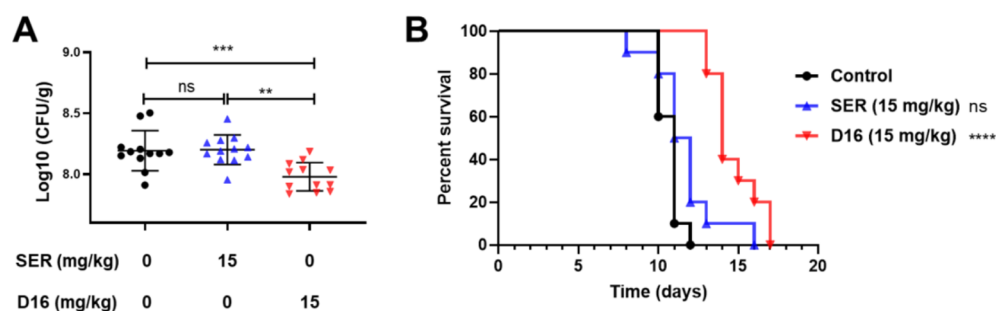


Figure 4. *In vivo* therapeutic effects of compound D16 in a *C. neoformans* H99-infected mouse model. (A) Fungal burden in the brain of infected mice. (B) Survival time assay of the mouse infection model. ns, not significant. ** $P < 0.01$, *** $P < 0.001$, and **** $P < 0.0001$.

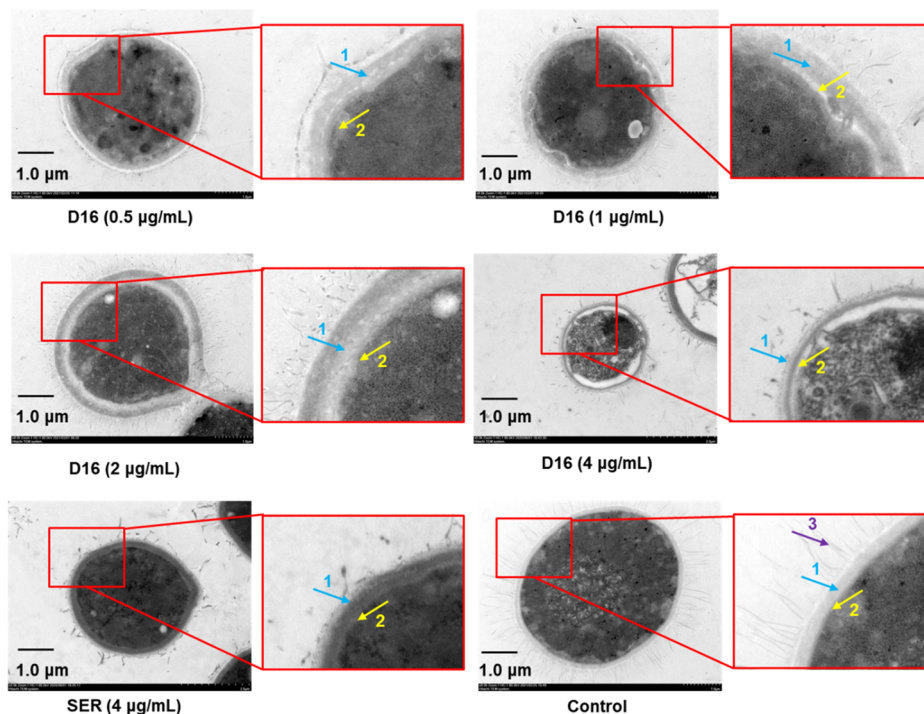


Figure 5. Transmission electron microscope micrographs of *C. neoformans* H99 under different conditions. The arrows indicate the following: (1) cell wall, (2) cell membrane, and (3) capsule.

spectrometry (GC-MS).³⁶ As shown in Figure 6A, the change in the sterol content of the compound D16 group was significantly different from those of the blank control, FLC, and SER groups. Analysis of five major sterols indicated that ergosta-7,22-dien-3-ol was the major sterol in the compound D16 group (Figure 6B). As compared with the blank control, compound D16 caused a substantial decrease in the level of ergosterol (Figure 6B). Furthermore, ergosta-7,22-dien-3-ol was increased in a concentration-dependent manner by treatment with compound D16 (Figure 6C). At concentrations of $<8 \mu\text{g/mL}$, SER had little effect in changing the sterol contents and ergosta-7,22-dien-3-ol could not be detected. When the concentration of SER was increased to $16 \mu\text{g/mL}$, the sterol content analysis was difficult because of the fungicidal effect of SER, and little ergosta-7,22-dien-3-ol was detected (Figure 6D). These results indicated that compound D16 acted by a new antifungal mechanism of action. It destroyed the cell membrane of *C. neoformans* H99 by inhibiting the biosynthesis of ergosterol, leading to the accumulation of ergosta-7,22-dien-3-ol. Notably, the mechanism was different from that of known antifungal drugs (FLC

and amorolfine) acting on the fungal cell membrane (Figures S1–S3).

Ergosta-7,22-dien-3-ol is the precursor of ergosterol in the *C. neoformans* H99 sterol biosynthesis pathway, which is transformed by $\Delta^{5,6}$ -desaturase [expressed by the *ERG3* gene (Figure 7A)].^{39–41} To further clarify whether compound D16 inhibited the $\Delta^{5,6}$ -desaturase of *C. neoformans* H99, total sterols of *C. neoformans* H99 cells were extracted after their treatment with $3 \mu\text{g/mL}$ compound D16, and then total *ERG* enzymes of *C. neoformans* H99 were added and interacted with the total sterols. GC-MS analysis revealed that ergosta-7,22-dien-3-ol could be transformed into ergosterol upon treatment with total *ERG* enzymes (Figure 7B,C). However, the transformation was reversed after treatment with compound D16. Therefore, compound D16 blocked the biosynthesis of ergosterol through the inhibition of $\Delta^{5,6}$ -desaturase.

Different Sterol Components between *C. albicans* SC5314 and *C. neoformans* H99 Caused the Selective Antifungal Potency of Compound D16. The *ERG3* gene in *C. albicans* is related to drug resistance and pathogenicity, and ergosta-7,22-dien-3-ol functions in the compensatory metabolic

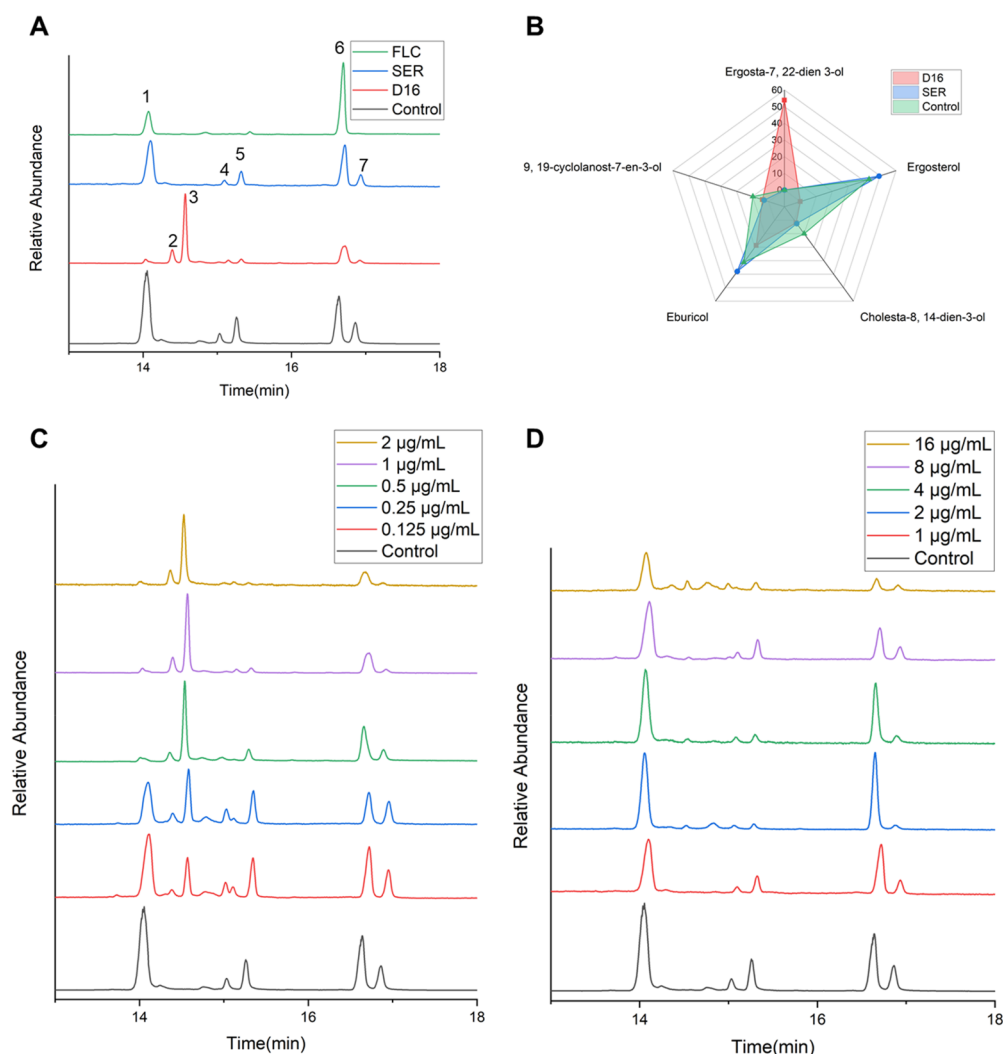


Figure 6. Analysis of the total sterol contents of *C. neoformans* H99. (A) Changes in ergosterol content in *C. neoformans* H99 after treatment with different drugs (2 $\mu\text{g/mL}$): (1) ergosterol, (2) unknown sterol, (3) ergosta-7,22-dien-3-ol, (4) ergost-7-en-3-ol, (5) cholesta-8,14-dien-3-ol, (6) eburicol, and (7) 9,19-cyclolanost-7-en-3-ol (each number corresponds to a substance; a matching score of >700 is considered to be quite reliable). (B) Changes in the content of the main sterols ($>10\%$) in *C. neoformans* H99 cells after treatment with compound D16 or SER (1 $\mu\text{g/mL}$). (C) Changes in ergosterol content in *C. neoformans* H99 cells after treatment with different concentrations of compound D16. (D) Changes in ergosterol content of *C. neoformans* H99 cells after treatment with different concentrations of SER.

pathway, which is not the key intermediate in *C. albicans* ergosterol synthesis.⁴² We further investigated the change in sterol content in *C. albicans* SC3514 after treatment with compound D16. Normally, the sterol contents of *C. neoformans* H99 and *C. albicans* SC3514 were different (Figure 8A). The effect of compound D16 on the sterol contents of *C. albicans* SC3514 was also different from those of *C. neoformans* H99. After treatment with compound D16, the ergosterol content of *C. albicans* SC3514 was decreased and only a very small amount of ergosta-7,22-dien-3-ol was produced. As a result, compound D16 has a selective inhibitory effect on *Cryptococcus*, possibly due to different compensatory pathways for ergosterol biosynthesis between *C. neoformans* H99 and *C. albicans* SC3514 (Figure 8B).

Compound D16 Upregulated *ERG*-Related Gene Expression. Transmission electron microscopy and sterol content analysis showed that the fungistatic potency of compound D16 against *C. neoformans* H99 was related to the biosynthetic pathway of ergosterol. Therefore, we further investigated the expression of related genes involved in

ergosterol biosynthesis. As shown in Figure 9A, all of the tested *ERG*-related genes were upregulated following treatment with FLC and compound D16. It has been reported that the ergosta-7,22-dien-3-ol was converted to ergosterol by the catalysis of $\Delta^{5,6}$ -desaturase (*ERG3* gene).^{41,43,44} The *ERG3* gene was upregulated in a concentration-dependent manner, which indicated that compound D16 inhibited the enzyme activity of $\Delta^{5,6}$ -desaturase, and then *C. neoformans* H99 upregulated the *ERG3* gene under stress. Similarly, *ERG11* was also upregulated in a concentration-dependent manner (Figure 9B,C). Although the expression of *ERG3* and *ERG11* genes of *C. albicans* SC3514 was also upregulated, the upregulation ratio was significantly lower than that of *C. neoformans* H99 (Figure 9D,E). The upregulated expression of the *ERG*-related genes in *C. neoformans* H99 indicated that compound D16 inhibited ergosterol biosynthesis, which resulted in stress-induced upregulation of *ERG* genes in *C. neoformans* H99.⁴⁵

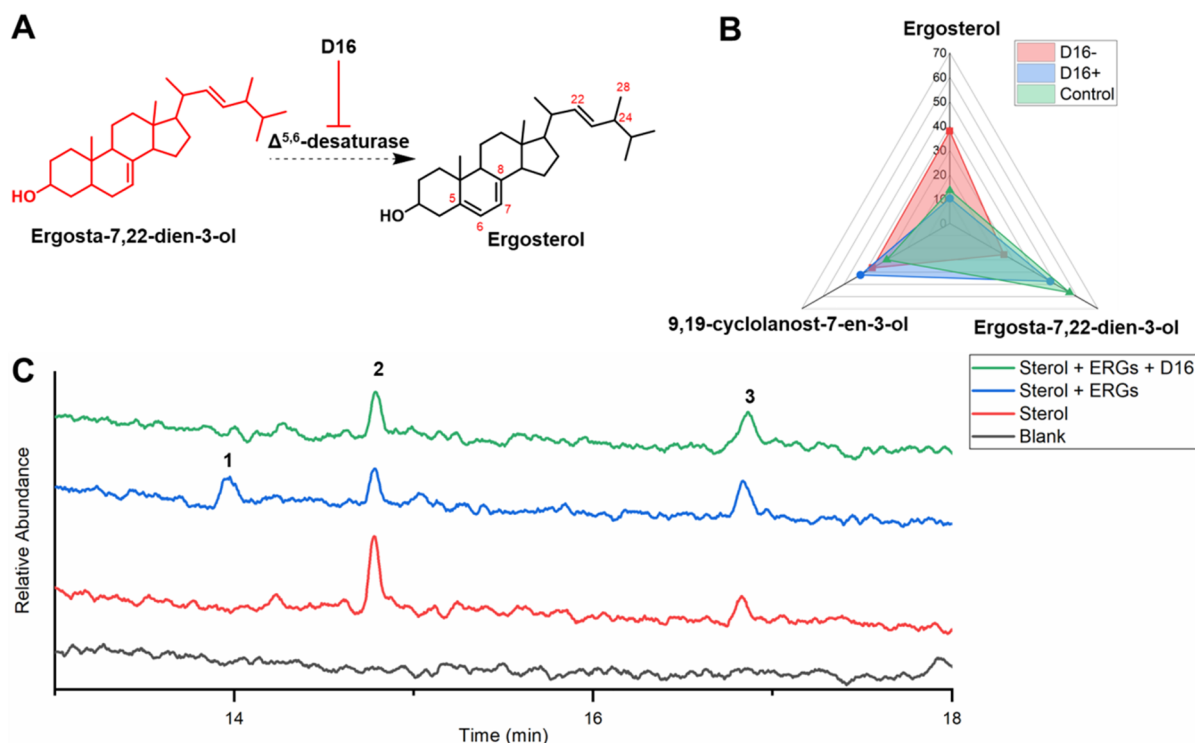


Figure 7. Compound **D16** inhibited $\Delta^{5,6}$ -desaturase of *C. neoformans* H99. (A) Partial pathway of ergosterol biosynthesis in *C. neoformans* H99. (B and C) Total sterols of *C. neoformans* H99 cells were extracted after their treatment with 3 $\mu\text{g/mL}$ compound **D16**. Transformation of ergosta-7,22-dien-3-ol by total ERG enzymes of *C. neoformans* H99 using total sterols after treatment with compound **D16** as the substrate. Compound **D16** (0.5 $\mu\text{g/mL}$) was added, and the mixture incubated for 24 h; the total sterol content was analyzed by GC-MS: (1) ergosterol, (2) ergosta-7,22-dien-3-ol, and (3) 9,19-cyclolanost-7-en-3-ol.

CONCLUSIONS

In summary, novel SER derivatives were designed and assayed. As compared with SER, compound **D16** showed improved antifungal potency both *in vitro* and *in vivo*. It had selective and fungistatic activity against *C. neoformans* H99 and completely inhibited biofilm formation at 8 $\mu\text{g/mL}$. In a mouse model of CM, compound **D16** effectively reduced the brain fungal burden and prolonged the survival time, which represented a promising candidate for the treatment of CM. Interestingly, compound **D16** acted by a new antifungal mechanism, which inhibited the activity of $\Delta^{5,6}$ -desaturase and blocked the transformation of ergosta-7,22-dien-3-ol to ergosterol, leading to the rupture of the *C. neoformans* H99 cell membrane. Thus, $\Delta^{5,6}$ -desaturase holds promise as a new target for antifungal drug discovery. Further mechanistic validation, antifungal evaluations, and structural optimizations are currently in progress.

EXPERIMENTAL SECTION

General Chemistry Methods. The reagents and solvents were all chemically or analytically pure. A GF254 silica gel plate (Qingdao Haiyang Chemical Co.) was used for TLC analysis, and 300–400 mesh silica gel was used for column chromatography (Qingdao Haiyang Chemical Co.). A Bruker AVANCE 300 or Bruker AVANCE 600 spectrometer was used for NMR analysis (Bruker), with TMS as the internal standard and CDCl_3 or $\text{DMSO}-d_6$ as the solvent. Chemical shifts (δ) and coupling constants (J) are expressed in parts per million and hertz, respectively. A model API-3000 LC-MS mass spectrometer was used for mass spectrometry analysis. An Agilent 1260 high-performance liquid chromatograph was used for purity determination, and the purities of all target compounds were >95%.

7-(3-Dichlorophenyl)-N-[2-(tetrahydro-2-muran-pyran-4-yl)ethyl]-4-tetrahydrobenzo[b]thiophene-4-amine Hydro-

chloride (D16). Intermediate **7a** (106 mg, 0.36 mmol), 2-(tetrahydro-2H-pyran-4-yl)ethan-1-amine (93 mg, 0.72 mmol), tetraisopropyl titanate (307 mg, 1.08 mmol), and sodium cyanoborohydride (159 mg, 2.52 mmol) were dissolved in 50 mL of methanol, and then the mixture was stirred overnight at 40 $^{\circ}\text{C}$. The reaction was quenched with water, and then the mixture was filtered and extracted with EtOAc (3×30 mL). The combined organic layers were washed with saturated brine (3×30 mL) and dried with anhydrous Na_2SO_4 . Then, the mixture was filtered and concentrated under reduced pressure. The crude product was separated by column chromatography [100/1 (v/v) DCM/methanol] to afford a colorless oil; the colorless oil was dissolved in DCM, 1 mL of a hydrochloric acid/diethyl ether solution added at room temperature, and the mixture stirred for 1 h. The mixture was concentrated under reduced pressure to afford target compound **D16** as a white powder (37 mg, 23.3%): ^1H NMR of diastereomer 1 (600 MHz, $\text{DMSO}-d_6$) δ 9.29 (s, 1H), 9.18 (s, 1H), 7.61 (d, J = 8.3 Hz, 1H), 7.52 (d, J = 5.3 Hz, 1H), 7.50–7.48 (m, 2H), 7.19 (dd, J = 8.4, 2.1 Hz, 1H), 4.60–4.52 (m, 1H), 4.33–4.28 (m, 1H), 3.85–3.81 (m, 2H), 3.30–3.28 (m, 1H), 3.28–3.26 (m, 1H), 3.08–2.94 (m, 2H), 2.36–2.29 (m, 1H), 2.25–2.21 (m, 1H), 1.96–1.89 (m, 2H), 1.69–1.59 (m, 5H), 1.21–1.12 (m, 2H); ^1H NMR of diastereomer 2 (600 MHz, $\text{DMSO}-d_6$) δ 9.18 (s, 1H), 9.11 (s, 1H), 7.67 (d, J = 2.0 Hz, 1H), 7.63 (d, J = 8.3 Hz, 1H), 7.51–7.49 (m, 1H), 7.41 (dd, J = 8.3, 2.1 Hz, 1H), 7.37 (d, J = 5.3 Hz, 1H), 4.45–4.39 (m, 1H), 4.25–4.21 (m, 1H), 3.85–3.81 (m, 2H), 3.33–3.28 (m, 1H), 3.17–3.07 (m, 1H), 2.98–2.90 (m, 2H), 2.29–2.23 (m, 1H), 2.19–2.12 (m, 1H), 2.11–2.05 (m, 1H), 2.05–2.00 (m, 1H), 1.69–1.59 (m, 5H), 1.25–1.18 (m, 2H); ^{13}C NMR of diastereomer 1 (150 MHz, $\text{DMSO}-d_6$) δ 146.51, 144.95, 132.35, 131.54, 131.13, 130.37, 130.05, 128.75, 126.96, 125.82, 67.32, 52.69, 41.72, 41.07, 40.55, 32.87, 32.72, 32.47, 30.16, 23.98; ^{13}C NMR of diastereomer 2 (150 MHz, $\text{DMSO}-d_6$) δ 146.27, 143.93, 132.03, 131.52, 131.00, 130.63, 130.11, 129.33, 128.15, 125.52, 67.29, 51.50, 43.13, 41.83, 32.84, 32.78, 32.63, 28.14, 24.23; HRMS (ESI, positive) m/z calcd for $\text{C}_{21}\text{H}_{25}\text{Cl}_2\text{NOS}$ [$\text{M} + \text{H}$] $^+$ 410.1107, found 410.1118; HPLC purity 97.05% (total purity of

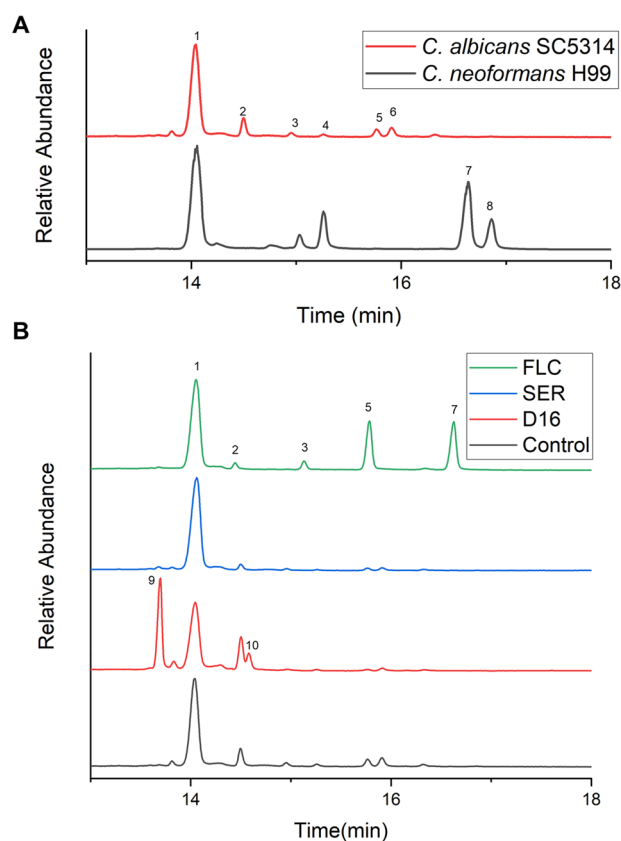


Figure 8. Analysis of the total sterol contents of *C. albicans* SC5314. (A) Comparison of sterol components between *C. albicans* SC5314 and *C. neoformans* H99. (B) Changes in the ergosterol contents of *C. albicans* SC5314 after treatment with different drugs (2 μg/mL): (1) ergosterol, (2) ergosta-5,24(28)-dien-3-ol, (3) desmosterol, (4) unknown sterol, (5) lanosterol, (6) cholesta-7,9(11)-dien-3-ol, (7) eburicol, (8) 9,19-cyclolanost-7-en-3-ol, (9) unknown sterol, and (10) ergosta-7,22-dien-3-ol.

diastereomers 1 and 2); retention time of 9.04 min, eluted with 60% methanol and 40% H₂O containing 0.1% TFA.

Preparation methods of target compounds **D1–15** and **D17–21** were the same as that of target compound **D16**.

N-(2-Cyclohexylethyl)-7-(3,4-dichlorophenyl)-4,5,6,7-tetrahydrobenzo[b]thiophen-4-amine Hydrochloride (D14). White powder (47 mg, 31.4%); ¹H NMR of diastereomer 1 (600 MHz, DMSO-*d*₆) δ 9.25 (s, 1H), 9.13 (s, 1H), 7.61 (d, *J* = 8.3 Hz, 1H), 7.53 (dd, *J* = 5.3, 0.6 Hz, 1H), 7.50 (d, *J* = 2.1 Hz, 1H), 7.49 (d, *J* = 5.3 Hz, 1H), 7.20 (dd, *J* = 8.4, 2.1 Hz, 1H), 4.59–4.53 (m, 1H), 4.32 (t, *J* = 6.2 Hz, 1H), 3.00–2.90 (m, 2H), 2.36–2.30 (m, 1H), 2.29–2.23 (m, 1H), 1.97–1.86 (m, 2H), 1.75–1.55 (m, 7H), 1.36–1.31 (m, 1H), 1.24–1.11 (m, 3H), 0.94–0.87 (m, 2H); ¹H NMR of diastereomer 2 (600 MHz, DMSO-*d*₆) δ 9.13 (s, 1H), 9.07 (s, 1H), 7.67 (d, *J* = 2.1 Hz, 1H), 7.64 (d, *J* = 8.3 Hz, 1H), 7.51 (dd, *J* = 5.3, 0.6 Hz, 1H), 7.42 (dd, *J* = 8.3, 2.1 Hz, 1H), 7.37 (d, *J* = 5.3 Hz, 1H), 4.45–4.40 (m, 1H), 4.24 (dd, *J* = 9.0, 5.4 Hz, 1H), 3.15–3.07 (m, 1H), 3.05–3.00 (m, 1H), 2.25–2.22 (m, 1H), 2.19–2.12 (m, 1H), 2.11–2.06 (m, 1H), 2.06–1.98 (m, 1H), 1.75–1.55 (m, 7H), 1.40–1.35 (m, 1H), 1.24–1.11 (m, 3H), 1.00–0.93 (m, 2H); ¹³C NMR of diastereomer 1 (150 MHz, DMSO-*d*₆) δ 146.50, 144.93, 132.33, 131.54, 131.13, 130.37, 130.05, 128.75, 126.86, 125.86, 52.69, 42.27, 41.05, 35.15, 33.34, 33.01, 32.73, 30.10, 26.03, 23.96; ¹³C NMR of diastereomer 2 (150 MHz, DMSO-*d*₆) δ 146.26, 143.93, 132.02, 131.52, 131.01, 130.60, 130.12, 129.31, 128.08, 125.57, 51.53, 43.68, 41.79, 35.42, 33.24, 32.97, 32.84, 28.12, 26.35, 24.22; HRMS (ESI, positive) *m/z* calcd for C₂₂H₂₈Cl₂NS [M + H]⁺ 408.1314, found 408.1318.

Strains, Culture, and Reagents. The sources of strains are listed in Table S5. A monoclonal fungal colony was placed in 1 mL of yeast extract peptone dextrose (YEPD) medium (1% yeast extract, 2% peptone, and 2% dextrose) and incubated in a shaker for 16 h (30 °C and 200 rpm). The fungal suspension was centrifuged (3000 rpm for 1 min), and then the supernatant was removed. The fungal cells were washed three times with PBS before being used. All of the target compounds were prepared as 2 mg/mL solutions with DMSO.

In Vitro Antifungal Activity Assay. The microdilution method was that of the Clinical and Laboratory Standards Institute (M27-A3).^{46,47} In brief, the fungal cells at the exponential growth stage were diluted to a density of 1 × 10⁵ cells/mL with RPMI 1640 medium. Different concentrations of target compounds and FLC were added to the fungal suspension, and it was serially diluted 2-fold. The fungal solution was cultured at 35 °C (*Cryptococcus* for 72 h and other fungi for 48 h), and the OD₆₃₀ was measured with a microplate reader. The lowest drug concentration that reduced the level of fungal growth by >50% was expressed by IC₅₀ in a single strain.⁴⁸ The MIC₅₀ value was the average of the IC₅₀ values against 50 *Cryptococcus* strains.⁴⁹ MIC was the average value of the lowest concentration that inhibits ≥90% (no visible growth) of 50 strains of *Cryptococcus*.⁵⁰

Time-Growth Curve Assay. *C. neoformans* H99 cells were diluted to a density of 1 × 10⁶ cells/mL with RPMI 1640 medium. Different concentrations of FLC, SER, and compounds **D14** and **D16** were added to the *C. neoformans* H99 suspension. The untreated group was used as the negative control group. Different samples were cultured at 30 °C. At set times (0, 4, 8, 12, 24, 48, and 72 h), the *C. neoformans* H99 suspension (100 μL) was sacked and the OD₆₃₀ value was measured with a microplate reader.

Time-Fungicidal Curve Assay. *C. neoformans* H99 cells were diluted to a density of 1 × 10⁵ CFU/mL with RPMI 1640 medium. Different concentrations of AmB, SER, FLC, and compound **D16** were added to the *C. neoformans* H99 suspension. The untreated group was used as the negative control group. Different samples were cultured at 30 °C. At set times (0, 4, 8, 12, 24, 48, and 72h), the suspension was coated on the SDA plate and incubated at 30 °C. The number of monoclonal fungal colonies on the plate was counted. MFC was defined as a 99.9% reduction in CFU from the starting fungal concentration.

Biofilm Formation Inhibition Assay. *C. neoformans* H99 cells were diluted to a density of 1 × 10⁵ cells/mL in RPMI 1640 medium. The suspension was added to a 96-well tissue culture plate (Corning, catalog no. 3599) and cultured at 37 °C for 180 min. After that, the RPMI 1640 medium was removed. Different concentrations of FLC, SER, and compounds **D14** and **D16** prepared with RPMI 1640 medium were added, and the plates were incubated at 37 °C for 24 h. The semiquantitative determination of biofilm formation was carried out by XTT reduction analysis, and the significant differences among the groups were analyzed by a Student's *t* test.

In Vivo Anti-Cryptococcal Assay. The animal study was approved by the Animal Ethics use Committee of the Second Military Medical University. ICR female mice (18–22 g, 4–6 weeks of age) were reared for 7 days before being inoculated for acclimatization. Each mouse was injected with 1 × 10⁶ *C. neoformans* H99 cells by tail vein injection. Compound **D16** and SER (suspended in 98% normal saline, 1.5% glycerol, and 0.5% Tween 80) were intragastrically administered for 5 days at a dose of 15 mg/kg. The control group was treated with normal saline. The mice were sacrificed, and brains were removed on the sixth day. The brains were ground and diluted with 1 mL of normal saline, and then the homogenate was diluted with different proportions and coated on the prepared SDA plate (including 100 μg/mL chloramphenicol). The number of monoclonal colonies on the plate was counted, and the significant differences between the groups were subjected to analysis of variance (ANOVA). The mouse survival time assay was performed using a similar protocol, and the survival time of mice was recorded. The significant difference between the groups was analyzed by the log-rank test.

Transmission Electron Microscope Assay. Transmission electron microscope images were obtained using the reported protocol.^{51,52} *C. neoformans* H99 cells were diluted with YEPD medium to a density of 5 × 10⁵ cells/mL. Compound **D16**, SER, FLC, and

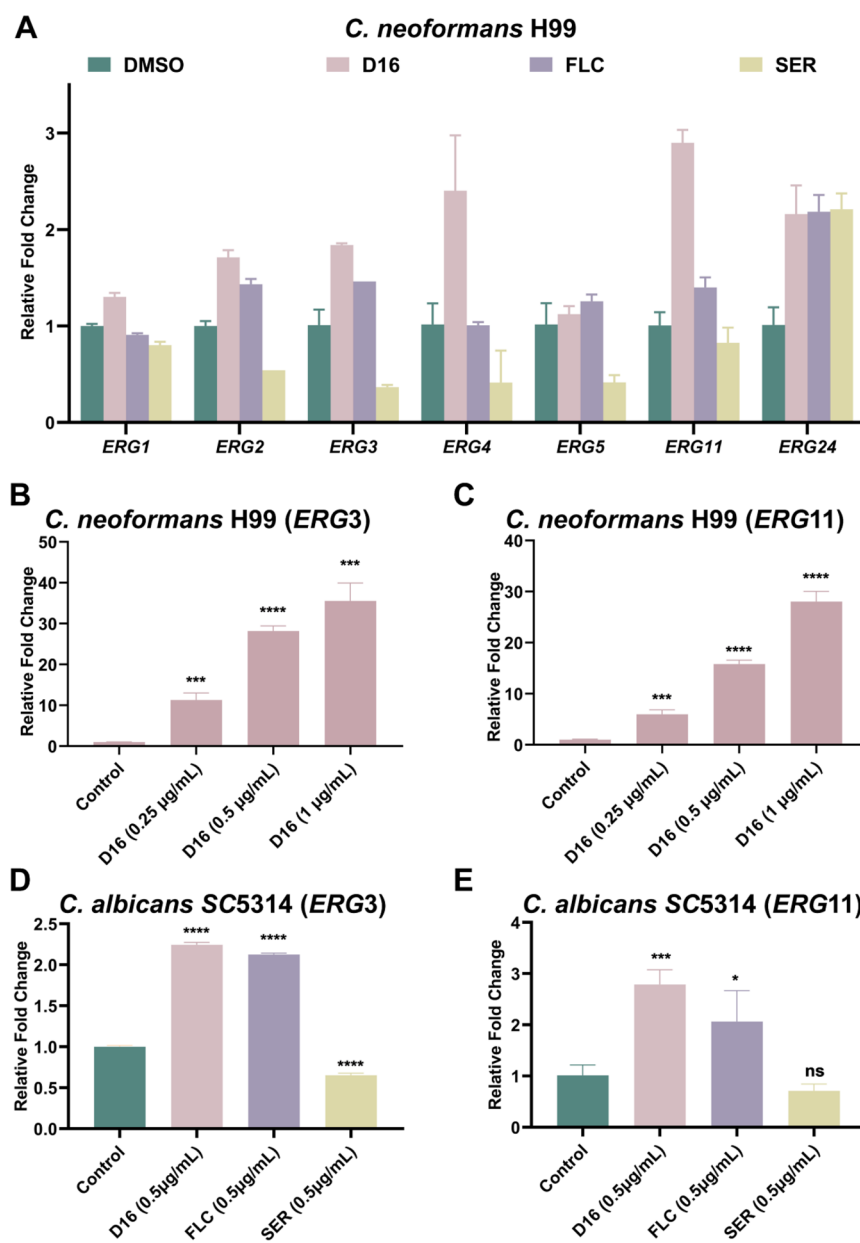


Figure 9. Expression of *ERG* genes in *C. neoformans* H99 and *C. albicans* SC5314 after their treatment with compound **D16**, **SER**, and **FLC**. (A) Expression of *ERG* genes in *C. neoformans* H99 treated with compound **D16**, **SER**, and **FLC** at 2 μ g/mL. (B and C) Expression of *ERG3* and *ERG11* genes, respectively, in *C. neoformans* H99 cells treated with different concentrations of compound **D16**. (D and E) Expression of *ERG3* and *ERG11* genes, respectively, in *C. albicans* SC5314 cells treated with compound **D16**, **SER**, and **FLC** at 2 μ g/mL. ns, not significant. * P < 0.05, ** P < 0.01, *** P < 0.001, and **** P < 0.0001 vs DMSO.

DMSO were added to the suspension as different groups, and then the suspension was cultured at 30 °C for 8 h. The suspension was washed three times with PBS, an electron microscope fixing solution (4% paraformaldehyde) was added to the suspension, and the suspension fixed overnight at 4 °C. The samples were washed with PBS and fixed for 90 min in 1% phosphotungstic acid. The fixed cells were dehydrated and embedded in EPON-812. The prepared ultrathin sections were double stained with uranium and lead, and then each sample was observed under a transmission electron microscope (Hitachi H-800) at 10⁴× magnification.

Fungal Sterol Composition Analysis. Fungi were added to YEPD medium (50 mL) to prepare a suspension with a concentration of 1 × 10⁶ cells/mL. Different groups were cultured at 30 °C for 24 h. After that, fungus cells were collected, washed twice with PBS, and saponified with 10 mL of a saponifier (90% ethanol solution containing 15% NaOH) at 80 °C for 1 h. The precipitate was extracted three times

with 4 mL of hexane; then the hexane was removed under reduced pressure, and the residue was dissolved with 400 μ L of cyclohexane. The sterols were analyzed by GC-MS. The sterols were identified by using the National Institute of Standards and Technology (NIST) reference database.

Inhibition Assay of the Total *ERG* Enzyme. A monoclonal *C. neoformans* H99 colony was placed in 1 mL of YEPD medium and incubated in a shaker for 16 h at 37 °C, and then the *C. neoformans* H99 cells were washed three times with PBS and weighed. Snailase was added to break the cell wall for 3 h (3 mL of snailase reaction buffer, 250 μ L of snailase, and 12 μ L of 2-hydroxy-1-ethanethiol per 100 mg of fungi). Then, the total *C. neoformans* H99 enzyme was obtained. Total sterols of *C. neoformans* H99 cells were extracted after treatment with compound **D16** at 3 μ g/mL. Total *ERG* enzymes, compound **D16**, and total sterols were added to reaction buffer [50 mM Tris-HCl (pH 7.4), 150 mM KCl, 10 mM MgCl₂, and 2 mM NADPH].⁵³ The samples were

incubated at 37 °C for 24 h. The transformation of sterol was analyzed by GC-MS.

Real Time RT-PCR Assay. The real time RT-PCR assay was performed according to previously described protocols.^{4,46,54} A fungal suspension was added to the YEPD medium to afford a density of 1×10^6 cells/mL. Compound **D16**, SER, FLC, and DMSO were added to the suspension as different groups, and then the fungal suspension was cultured at 30 °C for 24 h. Fungal cells were collected, and RNA of fungi was extracted according to the instructions of the kit (RNeasy Plant Mini kit, QIAGEN). The cDNA was obtained by reverse transcription by a reverse transcription kit (TaKaRa Biotechnology). The primer sequences are listed in Table S4. RT-PCR analysis was performed by using the StepOne System Fast real time PCR (Applied Biosystems). *ACTIN* was used as an internal control gene. The level of gene expression was expressed as multiple changes ($2^{-\Delta\Delta C_T}$ method), and the assay was performed in triplicate.

■ ASSOCIATED CONTENT

SI Supporting Information

The Supporting Information is available free of charge at <https://pubs.acs.org/doi/10.1021/acs.jmedchem.1c01845>.

Antifungal activity of compound **D16** against 50 strains of *Cryptococcus*; MFC/MIC ratios of compound **D16**, SER, and AmB; BBB penetration in the PAMPA-BBB assay of FLC, SER, and compound **D16**; experimental procedure of the cytotoxicity assay; changes of the ergosterol content of *C. neoformans* H99 treated with different concentrations of FLC and amorolfine; comparison of sterol components of *C. neoformans* H99 treated with FLC, SER, and amorolfine at 2 µg/mL; sequences of primers in the RT-PCR assay; sources of strains; structural characterization of intermediates and target compounds; and HPLC spectra of compound **D16** (PDF)

Molecular formula strings of the target compounds (CSV)

■ AUTHOR INFORMATION

Corresponding Authors

Chunquan Sheng – Department of Medicinal Chemistry, School of Pharmacy, Second Military Medical University, Shanghai 200433, China; orcid.org/0000-0001-9489-804X; Phone: +86 21 81871201; Email: shengcq@smmu.edu.cn

Na Liu – Department of Medicinal Chemistry, School of Pharmacy, Second Military Medical University, Shanghai 200433, China; orcid.org/0000-0002-3920-1008; Phone: +86 21 81871230; Email: liuna@smmu.edu.cn

Jian Li – School of Pharmacy, East China University of Science & Technology, Shanghai 200237, People's Republic of China; orcid.org/0000-0002-7521-8798; Phone: +86 21 64252584; Email: jianli@ecust.edu.cn

Authors

Wang Li – Department of Medicinal Chemistry, School of Pharmacy, Second Military Medical University, Shanghai 200433, China

Zhaolin Yun – Department of Medicinal Chemistry, School of Pharmacy, Second Military Medical University, Shanghai 200433, China

Changjin Ji – School of Pharmacy, East China University of Science & Technology, Shanghai 200237, People's Republic of China

Jie Tu – Department of Medicinal Chemistry, School of Pharmacy, Second Military Medical University, Shanghai 200433, China

Wanzhen Yang – Department of Medicinal Chemistry, School of Pharmacy, Second Military Medical University, Shanghai 200433, China

Complete contact information is available at:

<https://pubs.acs.org/doi/10.1021/acs.jmedchem.1c01845>

Author Contributions

[§]W.L. and Z.Y. contributed equally to this work.

Notes

The authors declare no competing financial interest.

■ ACKNOWLEDGMENTS

This work was supported by the National Natural Science Foundation of China (Grants 81725020 to C.S., 81973175 to N.L., and 82003591 to J.T.), the Innovation Program of Shanghai Municipal Education Commission (Grant 2019-01-07-00-07-E00073 to C.S.), and the Science and Technology Commission of Shanghai Municipality (Grant 20S11900400 to C.S.).

■ ABBREVIATIONS USED

5-FU, 5-fluorouracil; AmB, amphotericin B; ANOVA, analysis of variance; ATCC, American Type Culture Collection; BBB, blood–brain barrier; CFU, colony forming units; CM, cryptococcal meningitis; CNS, central nervous system; DMSO, dimethyl sulfoxide; FLC, fluconazole; GC-MS, gas chromatography-mass spectrometry; HUVECs, human umbilical vein endothelial cells; ICR, Institute of Cancer Research; MFC, minimum fungicidal concentration; MIC, minimum inhibitory concentration; NIST, National Institute of Standards and Technology; PAMP, parallel artificial membrane permeability; RT-qPCR, quantitative reverse transcription PCR; SER, sertraline; SERT, serotonin transporter; WHO, World Health Organization; XTT, 2,3-bis(2-hydroxyethylthio)naphthalene-1,4-dione

■ REFERENCES

- (1) Denning, D. W.; Bromley, M. J. Infectious Disease. How to bolster the antifungal pipeline. *Science* **2015**, *347*, 1414–1416.
- (2) Limper, A. H.; Adenis, A.; Le, T.; Harrison, T. S. Fungal infections in HIV/AIDS. *Lancet Infect. Dis.* **2017**, *17*, e334–e343.
- (3) Liu, W.; Yuan, L.; Wang, S. Recent progress in the discovery of antifungal agents targeting the cell wall. *J. Med. Chem.* **2020**, *63*, 12429–12459.
- (4) Li, Z.; Tu, J.; Han, G.; Liu, N.; Sheng, C. Novel carboline fungal histone deacetylase (HDAC) inhibitors for combinational treatment of azole-resistant candidiasis. *J. Med. Chem.* **2021**, *64*, 1116–1126.
- (5) Loyse, A.; Burry, J.; Cohn, J.; Ford, N.; Chiller, T.; Ribeiro, I.; Koulla-Shiro, S.; Mghamba, J.; Ramadhani, A.; Nyirenda, R.; Aliyu, S. H.; Wilson, D.; Le, T.; Oladele, R.; Lesikari, S.; Muzoora, C.; Kalata, N.; Temfack, E.; Mapoure, Y.; Sini, V.; Chanda, D.; Shimwela, M.; Lakhi, S.; Ngoma, J.; Gondwe-Chunda, L.; Perfect, C.; Shroufi, A.; Andrieux-Meyer, I.; Chan, A.; Schutz, C.; Hosseini-pour, M.; Van der Horst, C.; Klausner, J. D.; Boulware, D. R.; Heyderman, R.; Lalloo, D.; Day, J.; Jarvis, J. N.; Rodrigues, M.; Jaffar, S.; Denning, D.; Migone, C.; Doherty, M.; Lortholary, O.; Dromer, F.; Stack, M.; Molloy, S. F.; Bicanic, T.; van Oosterhout, J.; Mwaba, P.; Kanyama, C.; Kouanfack, C.; Mfinanga, S.; Govender, N.; Harrison, T. S. Leave no one behind: response to new evidence and guidelines for the management of cryptococcal meningitis in low-income and middle-income countries. *Lancet Infect. Dis.* **2019**, *19*, e143–e147.

- (6) Krystufek, R.; Sacha, P.; Starkova, J.; Brynda, J.; Hradilek, M.; Tloust'ova, E.; Grzyska, J.; Rut, W.; Boucher, M. J.; Drag, M.; Majer, P.; Hajek, M.; Rezacova, P.; Madhani, H. D.; Craik, C. S.; Konvalinka, J. Re-emerging aspartic protease targets: examining *Cryptococcus neoformans* major aspartyl peptidase 1 as a target for antifungal drug discovery. *J. Med. Chem.* **2021**, *64*, 6706–6719.
- (7) Zhang, F.; Zhao, M.; Braun, D. R.; Ericksen, S. S.; Piotrowski, J. S.; Nelson, J.; Peng, J.; Ananiev, G. E.; Chanana, S.; Barns, K.; Fossen, J.; Sanchez, H.; Chevette, M. G.; Guzei, I. A.; Zhao, C.; Guo, L.; Tang, W.; Currie, C. R.; Rajski, S. R.; Audhya, A.; Andes, D. R.; Bugni, T. S. A marine microbiome antifungal targets urgent-threat drug-resistant fungi. *Science* **2020**, *370*, 974–978.
- (8) Rajasingham, R.; Smith, R. M.; Park, B. J.; Jarvis, J. N.; Govender, N. P.; Chiller, T. M.; Denning, D. W.; Loyse, A.; Boulware, D. R. Global burden of disease of HIV-associated cryptococcal meningitis: an updated analysis. *Lancet Infect. Dis.* **2017**, *17*, 873–881.
- (9) Iyer, K. R.; Revie, N. M.; Fu, C.; Robbins, N.; Cowen, L. E. Treatment strategies for cryptococcal infection: challenges, advances and future outlook. *Nat. Rev. Microbiol.* **2021**, *19*, 454–466.
- (10) Spitzer, M.; Robbins, N.; Wright, G. D. Combinatorial strategies for combating invasive fungal infections. *Virulence* **2017**, *8*, 169–185.
- (11) Berman, J.; Krysan, D. J. Drug resistance and tolerance in fungi. *Nat. Rev. Microbiol.* **2020**, *18*, 319–331.
- (12) Lee, Y.; Puumala, E.; Robbins, N.; Cowen, L. E. Antifungal drug resistance: molecular mechanisms in *Candida albicans* and beyond. *Chem. Rev.* **2021**, *121*, 3390–3411.
- (13) Perfect, J. R. The antifungal pipeline: a reality check. *Nat. Rev. Drug Discovery* **2017**, *16*, 603–616.
- (14) Wall, G.; Lopez-Ribot, J. L. Screening repurposing libraries for identification of drugs with novel antifungal activity. *Antimicrob. Agents Chemother.* **2020**, *64*, e00924–20.
- (15) Coelho, C.; Casadevall, A. Cryptococcal therapies and drug targets: the old, the new and the promising. *Cell. Microbiol.* **2016**, *18*, 792–799.
- (16) Ji, C.; Liu, N.; Tu, J.; Li, Z.; Han, G.; Li, J.; Sheng, C. Drug repurposing of haloperidol: discovery of new benzocyclohexane derivatives as potent antifungal agents against cryptococcosis and candidiasis. *ACS Infect. Dis.* **2020**, *6*, 768–786.
- (17) Wang, S.; Dong, G.; Sheng, C. Structural simplification of natural products. *Chem. Rev.* **2019**, *119*, 4180–4220.
- (18) Feng, H.; Hu, L.; Zhu, H.; Tao, L.; Wu, L.; Zhao, Q.; Gao, Y.; Gong, Q.; Mao, F.; Li, X.; Zhou, H.; Li, J.; Zhang, H. Repurposing antimycotic ciclopirox olamine as a promising anti-ischemic stroke agent. *Acta Pharm. Sin. B* **2020**, *10*, 434–446.
- (19) Iwata, M.; Hirose, L.; Kohara, H.; Liao, J. Y.; Sawada, R.; Akiyoshi, S.; Tani, K.; Yamanishi, Y. Pathway-based drug repositioning for cancers: computational prediction and experimental validation. *J. Med. Chem.* **2018**, *61*, 9583–9595.
- (20) Gowri, M.; Jayashree, B.; Jeyakanthan, J.; Girija, E. K. Sertraline as a promising antifungal agent: inhibition of growth and biofilm of *Candida auris* with special focus on the mechanism of action in vitro. *J. Appl. Microbiol.* **2020**, *128*, 426–437.
- (21) Trevino-Rangel, R. J.; Villanueva-Lozano, H.; Mendez-Galomo, K. S.; Solis-Villegas, E. M.; Becerril-Garcia, M. A.; Montoya, A. M.; Robledo-Leal, E. R.; Gonzalez, G. M. In vivo evaluation of the antifungal activity of sertraline against *Aspergillus fumigatus*. *J. Antimicrob. Chemother.* **2019**, *74*, 663–666.
- (22) Lass-Flörl, C.; Dierich, M. P.; Fuchs, D.; Semenitz, E.; Ledochowski, M. Antifungal activity against *Candida* species of the selective serotonin-reuptake inhibitor, sertraline. *Clin. Infect. Dis.* **2001**, *33*, e135–e136.
- (23) Rhein, J.; Huppler Hullsiek, K.; Tugume, L.; Nuwagira, E.; Mpoza, E.; Evans, E. E.; Kiggundu, R.; Pastick, K. A.; Ssebambulidde, K.; Akampurira, A.; Williams, D. A.; Bangdiwala, A. S.; Abassi, M.; Musubire, A. K.; Nicol, M. R.; Muzoora, C.; Meza, D. B.; Boulware, D. R.; team, A.-C.; et al. Adjunctive sertraline for HIV-associated cryptococcal meningitis: a randomised, placebo-controlled, double-blind phase 3 trial. *Lancet Infect. Dis.* **2019**, *19*, 843–851.
- (24) Rhein, J.; Morawski, B. M.; Hullsiek, K. H.; Nabeta, H. W.; Kiggundu, R.; Tugume, L.; Musubire, A.; Akampurira, A.; Smith, K. D.; Alhadab, A.; Williams, D. A.; Abassi, M.; Bahr, N. C.; Velamakanni, S. S.; Fisher, J.; Nielsen, K.; Meza, D. B.; Boulware, D. R.; Team, A.-C. S. Efficacy of adjunctive sertraline for the treatment of HIV-associated cryptococcal meningitis: an open-label dose-ranging study. *Lancet Infect. Dis.* **2016**, *16*, 809–818.
- (25) Rosenberg, A.; Ene, I. V.; Bibi, M.; Zakin, S.; Segal, E. S.; Ziv, N.; Dahan, A. M.; Colombo, A. L.; Bennett, R. J.; Berman, J. Antifungal tolerance is a subpopulation effect distinct from resistance and is associated with persistent candidemia. *Nat. Commun.* **2018**, *9*, 2470.
- (26) Rainey, M. M.; Korostyshevsky, D.; Lee, S.; Perlstein, E. O. The antidepressant sertraline targets intracellular vesiculogenic membranes in yeast. *Genetics* **2010**, *185*, 1221–1233.
- (27) Costa Silva, R. A.; da Silva, C. R.; de Andrade Neto, J. B.; da Silva, A. R.; Campos, R. S.; Sampaio, L. S.; do Nascimento, F.; da Silva Gaspar, B.; da Cruz Fonseca, S. G.; Josino, M. A. A.; Grangeiro, T. B.; Gaspar, D. M.; de Lucena, D. F.; de Moraes, M. O.; Cavalcanti, B. C.; Nobre Junior, H. V. In vitro anti-candida activity of selective serotonin reuptake inhibitors against fluconazole-resistant strains and their activity against biofilm-forming isolates. *Microb. Pathog.* **2017**, *107*, 341–348.
- (28) Krumlinde, P.; Bogar, K.; Backvall, J. E. Asymmetric synthesis of bicyclic diol derivatives through metal and enzyme catalysis: application to the formal synthesis of sertraline. *Chemistry* **2010**, *16*, 4031–4036.
- (29) Fustero, S.; Lazaro, R.; Herrera, L.; Rodriguez, E.; Mateu, N.; Barrio, P. Asymmetric allylation/ring closing metathesis: one-pot synthesis of benzo-fused cyclic homoallylic amines. Application to the formal synthesis of Sertraline derivatives. *Org. Lett.* **2013**, *15*, 3770–3773.
- (30) Koe, B. K.; Weissman, A.; Welch, W. M.; Browne, R. G. Sertraline, 1S,4S-N-methyl-4-(3,4-dichlorophenyl)-1,2,3,4-tetrahydro-1-naphthylamine, a new uptake inhibitor with selectivity for serotonin. *J. Pharmacol. Exp. Ther.* **1983**, *226*, 686–700.
- (31) Mu, C.; Peng, R. K.; Guo, C. L.; Li, A.; Yang, X. M.; Zeng, R.; Li, Y. L.; Gu, J.; Ouyang, Q. Discovery of sertraline and its derivatives able to combat drug-resistant gastric cancer cell via inducing apoptosis. *Bioorg. Med. Chem. Lett.* **2021**, *41*, 127997.
- (32) Li, Z.; Liu, N.; Tu, J.; Ji, C.; Han, G.; Wang, Y.; Sheng, C. Discovery of novel simplified isoxazole derivatives of sampangine as potent anti-cryptococcal agents. *Bioorg. Med. Chem.* **2019**, *27*, 832–840.
- (33) Koo, H.; Allan, R. N.; Howlin, R. P.; Stoodley, P.; Hall-Stoodley, L. Targeting microbial biofilms: current and prospective therapeutic strategies. *Nat. Rev. Microbiol.* **2017**, *15*, 740–755.
- (34) Wang, S.; Wang, Y.; Liu, W.; Liu, N.; Zhang, Y.; Dong, G.; Liu, Y.; Li, Z.; He, X.; Miao, Z.; Yao, J.; Li, J.; Zhang, W.; Sheng, C. Novel carboline derivatives as potent antifungal lead compounds: design, synthesis, and biological evaluation. *ACS Med. Chem. Lett.* **2014**, *5*, 506–511.
- (35) Liu, N.; Tu, J.; Dong, G.; Wang, Y.; Sheng, C. Emerging new targets for the treatment of resistant fungal infections. *J. Med. Chem.* **2018**, *61*, 5484–5511.
- (36) Muller, C.; Binder, U.; Bracher, F.; Giera, M. Antifungal drug testing by combining minimal inhibitory concentration testing with target identification by gas chromatography-mass spectrometry. *Nat. Protoc.* **2017**, *12*, 947–963.
- (37) Zakula, D.; Capobianco, J. O.; Goldman, R. C. Novel antifungal agents which inhibit lanosterol 14 α -demethylase in *Candida albicans* CCH442. *J. Antimicrob. Chemother.* **1997**, *39*, 261–264.
- (38) Liu, N.; Zhong, H.; Tu, J.; Jiang, Z.; Jiang, Y.; Jiang, Y.; Jiang, Y.; Li, J.; Zhang, W.; Wang, Y.; Sheng, C. Discovery of simplified sampangine derivatives as novel fungal biofilm inhibitors. *Eur. J. Med. Chem.* **2018**, *143*, 1510–1523.
- (39) Singh, A.; MacKenzie, A.; Girmun, G.; Del Poeta, M. Analysis of sphingolipids, sterols, and phospholipids in human pathogenic *Cryptococcus* strains. *J. Lipid Res.* **2017**, *58*, 2017–2036.
- (40) Nes, W. D.; Zhou, W.; Ganapathy, K.; Liu, J.; Vatsyayan, R.; Chamala, S.; Hernandez, K.; Miranda, M. Sterol 24-C-methyltransfer-

ase: an enzymatic target for the disruption of ergosterol biosynthesis and homeostasis in *Cryptococcus neoformans*. *Arch. Biochem. Biophys.* **2009**, *481*, 210–218.

(41) Oliveira, F. F. M.; Paes, H. C.; Peconick, L. D. F.; Fonseca, F. L.; Marina, C. L. F.; Bocca, A. L.; Homem-de-Mello, M.; Rodrigues, M. L.; Albuquerque, P.; Nicola, A. M.; Alspaugh, J. A.; Felipe, M. S. S.; Fernandes, L. Erg6 affects membrane composition and virulence of the human fungal pathogen *Cryptococcus neoformans*. *Fungal Genet. Biol.* **2020**, *140*, 103368.

(42) Lv, Q. Z.; Yan, L.; Jiang, Y. Y. The synthesis, regulation, and functions of sterols in *Candida albicans*: Well-known but still lots to learn. *Virulence* **2016**, *7*, 649–659.

(43) Revankar, S. G.; Fu, J.; Rinaldi, M. G.; Kelly, S. L.; Kelly, D. E.; Lamb, D. C.; Keller, S. M.; Wickes, B. L. Cloning and characterization of the lanosterol 14 α -demethylase (ERG11) gene in *Cryptococcus neoformans*. *Biochem. Biophys. Res. Commun.* **2004**, *324*, 719–728.

(44) Toh-e, A.; Ohkusu, M.; Shimizu, K.; Yamaguchi, M.; Ishiwada, N.; Watanabe, A.; Kamei, K. Creation, characterization and utilization of *Cryptococcus neoformans* mutants sensitive to micafungin. *Curr. Genet.* **2017**, *63*, 1093–1104.

(45) Li, Q. Q.; Tsai, H. F.; Mandal, A.; Walker, B. A.; Noble, J. A.; Fukuda, Y.; Bennett, J. E. Sterol uptake and sterol biosynthesis act coordinately to mediate antifungal resistance in *Candida glabrata* under azole and hypoxic stress. *Mol. Med. Rep.* **2018**, *17*, 6585–6597.

(46) Zhu, T.; Chen, X.; Li, C.; Tu, J.; Liu, N.; Xu, D.; Sheng, C. Lanosterol 14 α -demethylase (CYP51)/histone deacetylase (HDAC) dual inhibitors for treatment of *Candida tropicalis* and *Cryptococcus neoformans* infections. *Eur. J. Med. Chem.* **2021**, *221*, 113524.

(47) Tu, J.; Li, Z.; Jiang, Y.; Ji, C.; Han, G.; Wang, Y.; Liu, N.; Sheng, C. Discovery of carboline derivatives as potent antifungal agents for the treatment of cryptococcal meningitis. *J. Med. Chem.* **2019**, *62*, 2376–2389.

(48) Cruz, M. C.; Bartlett, M. S.; Edlind, T. In vitro susceptibility of the opportunistic fungus *Cryptococcus neoformans* to anthelmintic benzimidazoles. *Antimicrob. Agents Chemother.* **1994**, *38*, 378–380.

(49) Nixon, G. L.; McEntee, L.; Johnson, A.; Farrington, N.; Whalley, S.; Livermore, J.; Natal, C.; Washbourn, G.; Bibby, J.; Berry, N.; Lestner, J.; Truong, M.; Owen, A.; Laloo, D.; Charles, I.; Hope, W. Repurposing and reformulation of the antiparasitic agent flubendazole for treatment of cryptococcal meningoencephalitis, a neglected fungal disease. *Antimicrob. Agents Chemother.* **2018**, *62*, e01909–01917.

(50) Ramachandran, R.; Shrivastava, M.; Narayanan, N. N.; Thakur, R. L.; Chakrabarti, A.; Roy, U. Evaluation of antifungal efficacy of three new cyclic lipopeptides of the class bacillomycin from *Bacillus subtilis* RLID 12.1. *Antimicrob. Agents Chemother.* **2018**, *62*, e01457–01417.

(51) Montès, B.; Mallié, M.; Jouvert, S.; Bastide, J. M. Morphological changes of *Candida albicans* induced by saperconazole. *Mycoses* **1991**, *34*, 287–292.

(52) Han, G.; Liu, N.; Li, C.; Tu, J.; Li, Z.; Sheng, C. Discovery of novel fungal lanosterol 14 α -Demethylase (CYP51)/histone deacetylase dual inhibitors to treat azole-resistant candidiasis. *J. Med. Chem.* **2020**, *63*, 5341–5359.

(53) An, Y.; Dong, Y.; Liu, M.; Han, J.; Zhao, L.; Sun, B. Novel naphthylamide derivatives as dual-target antifungal inhibitors: Design, synthesis and biological evaluation. *Eur. J. Med. Chem.* **2021**, *210*, 112991.

(54) Yang, W.; Tu, J.; Ji, C.; Li, Z.; Han, G.; Liu, N.; Li, J.; Sheng, C. Discovery of piperidol derivatives for combinational treatment of azole-resistant candidiasis. *ACS Infect. Dis.* **2021**, *7*, 650–660.

Recommended by ACS

Novel Triazoles with Potent and Broad-Spectrum Antifungal Activity In Vitro and In Vivo

Panhu Zhu, Minghua Yang, *et al.*

MAY 23, 2023
JOURNAL OF MEDICINAL CHEMISTRY

READ 

Membrane-Active Nonivamide Derivatives as Effective Broad-Spectrum Antimicrobials: Rational Design, Synthesis, and Biological Evaluation

Qionga Cai, Shuimu Lin, *et al.*

DECEMBER 13, 2022
JOURNAL OF MEDICINAL CHEMISTRY

READ 

Quinazolinone Compounds Have Potent Antiviral Activity against Zika and Dengue Virus

Md Ashraf-Uz-Zaman, Yongcheng Song, *et al.*

JULY 28, 2023
JOURNAL OF MEDICINAL CHEMISTRY

READ 

N'-Phenylacetohydrazide Derivatives as Potent Ebola Virus Entry Inhibitors with an Improved Pharmacokinetic Profile

Alfonso Garcia-Rubia, Carmen Gil, *et al.*

APRIL 06, 2023
JOURNAL OF MEDICINAL CHEMISTRY

READ 

Get More Suggestions >